MATHEMATICAL MODELING OF LOOP HEAT PIPES WITH MULTIPLE CAPILLARY PUMPS AND MULTIPLE CONDENSERS PART I – STEADY STATE SIMULATIONS

Triem T. Hoang
Tamara A. O'Connell
TTH Research Inc.
Laurel, MD

Jentung Ku
NASA Goddard Space Flight Center
Greenbelt, MD

ABSTRACT

Loop Heat Pipes (LHPs) have proven themselves as reliable and robust heat transport devices for spacecraft thermal control systems. So far, the LHPs in earth-orbit satellites perform very well as expected. Conventional LHPs usually consist of a single capillary pump for heat acquisition and a single condenser for heat rejection. Multiple pump/multiple condenser LHPs have shown to function very well in ground testing. Nevertheless, the test results of a dual pump/condenser LHP also revealed that the dual LHP behaved in a complicated manner due to the interaction between the pumps and condensers. Thus it is redundant to say that more research is needed before they are ready for 0-g deployment. One research area that perhaps compels immediate attention is the analytical modeling of LHPs, particularly the transient phenomena. Modeling a single pump/single condenser LHP is difficult enough. Only a handful of computer codes are available for both steady state and transient simulations of conventional LHPs. No previous effort was made to develop an analytical model (or even a complete theory) to predict the operational behavior of the multiple pump/multiple condenser LHP systems. The current research project offered a basic theory of the multiple pump/multiple condenser LHP operation. From it, a computer code was developed to predict the LHP saturation temperature in accordance with the system operating and environmental conditions.

INTRODUCTION

Most of the analytical modeling efforts focused on the temperature prediction of single pump/single condenser (conventional) LHPs after a *steady state* condition was reached [1, 2, 3]. In these steady state models, energy balance among the heat leak across the primary wick, return liquid subcooling, and environmental parasitics was generally utilized to determine the loop saturation temperature for a given set of operating and ambient conditions. Predictions made by the models, for the most part, correlated well with the corresponding test data.

A transient model for conventional LHPs was recently developed under the direction of NASA Goddard Space Flight Center [4]. The governing equations were, of course, derived from the basic conservation laws of mass, momentum and energy. However, observations of unique LHP operational characteristics during testing also assisted the formulation of the LHP theory. The transient LHP model (FORTRAN computer code) was independently verified by several users with different LHPs [5, 6, 7]. The predictions-versus-data comparison was outstanding (error bounds < 2°C) even under severe operating conditions (e.g. rapid change of power/sink). But perhaps more important than that, the computer runtime was extremely efficient taking less than 2 seconds for a 1.8GHz Pentium IV laptop computer to simulate 10 hours of LHP operation. It did not exhibit any kind of numerical instability, either.

In the follow-on research, it was therefore logical to extend the aforementioned transient LHP theory/model for the analytical simulation of the NASA/GSFC dual pump/condenser LHP system. As it turned out, the methodology in formulating the theory and deriving the governing equations was more or less straightforward (albeit tedious). But the mechanics of solving the equations became so complicated that a new computer code had to be written from scratch for the multiple pump/condenser LHPs. Two versions of the code were developed in the current project. The steady state version was completed and verified with available test data. It is therefore the main focus of this paper. The theory, governing equations, solution scheme, and data correlation will be presented. The transient version was also finished and currently in the process of data comparison and evaluation. The results will be presented at a public forum in the near future.

NOMENCLATURE

$A_C^{(i)}$ ≡ cross-sectional area of condenser i.
c_P ≡ liquid specific heat of working fluid.
$D_C^{(i)}$ ≡ inner diameter of condenser i.
$D_{I,W}^{(i)}$ ≡ wick inner diameter of pump i.
$D_{O,W}^{(i)}$ ≡ wick outer diameter of pump i.
$G_{R-A}^{(i)}$ ≡ thermal conductance from reservoir i to ambient.
$h_{2\varphi}$ ≡ film coefficient for two-phase pipe flow.
h_L ≡ film coefficient for single-phase pipe flow.
$k_W^{(i)}$ ≡ effective thermal conductivity of wick i.
$L_C^{(i)}$ ≡ length of condenser i.
$L_{C,2\varphi}^{(i)}$ ≡ two-phase length of condenser i.
$L_W^{(i)}$ ≡ length of wick i.
$\dot{m}_C^{(i)}$ ≡ mass flow rate in condenser i.
$\dot{m}_P^{(i)}$ ≡ mass flow rate in pump i.
N_C ≡ number of parallel condensers.
N_P ≡ number of parallel capillary pumps.
$\dot{Q}_2^{(i)}$ ≡ heat leak across wick i.
$\dot{Q}_{2,MAX}^{(i)}$ ≡ maximum heat leak across wick i.
$\dot{Q}_C^{(i)}$ ≡ heat removal by condensation in condenser i.
$\dot{Q}_P^{(i)}$ ≡ heat input to capillary pump i.
$\dot{Q}_C$ ≡ heat removal by condensation at condenser.
$\dot{Q}_{R-A}^{(i)}$ ≡ heat loss from reservoir i to ambient.
$\dot{Q}_{SC}^{(i)}$ ≡ return liquid subcooling to pump i.
$\dot{Q}_{SC,MAX}^{(i)}$ ≡ maximum return liq. subcooling to pump i.
$Re = \frac{4\dot{m}_C^{(i)}}{\pi D_C^{(i)} \mu}$ ≡ Reynolds number of fluid flow.
$T_{IN}^{(i)}$ ≡ temperature of return liquid to pump i.
T_{SAT} ≡ saturation temperature of LHP.
T_{SINK} ≡ sink temperature.
T_∞ ≡ ambient temperature.
x ≡ vapor quality in two-phase flow.

Greek

α ≡ local vapor volume fraction of two-phase flow.
ε ≡ porosity of primary wick.
μ_L ≡ liquid viscosity of working fluid.
μ_V ≡ vapor viscosity of working fluid.
ν_L ≡ liquid kinematic viscosity of working fluid.
ρ_L ≡ liquid density of working fluid.
ρ_V ≡ vapor density of working fluid.
λ ≡ latent heat of vaporization of working fluid.
Φ_L ≡ two-phase function.
ΔP_C ≡ pressure drop across condensers.
$\Delta P_{C,L}^{(i)}$ ≡ pressure drop in liquid portion of condenser i.
$\Delta P_{C,2\varphi}^{(i)}$ ≡ 2-phase pressure drop of condenser i.
$\Delta P_{FR}^{(i)}$ ≡ pressure drop across flow regulator i.
$\Delta P_W^{(i)}$ ≡ pressure drop across meniscus of wick i.
$\Delta T_W^{(i)}$ ≡ temperature difference across wick i.
$\left(\frac{\partial T}{\partial P}\right)_{SAT}$ ≡ slope of T_{SAT} versus P_{SAT} curve.

LHP GOVERNING EQUATIONS

The derivation of the governing equations for a multiple pump/condenser is broken into two independent parts. One is for the heat rejection and fluid flow distribution among the parallel condensers. Note that capillary flow regulators, placed downstream of the condensers, may be needed to prevent vapor blow-through in case of a severe flow imbalance. The other set of equations is for the energy balance in the parallel capillary pump/hydro-accumulator assemblies.

PARALLEL CONDENSERS

The equations for steady state heat rejection/fluid flow distribution among the LHP parallel condensers were derived from three following basic principles:

- pressure drop across each condenser is identical.
- mass flow rate in a condenser is exactly equal to the condensation rate of heat removal.
- when a condenser is fully open, the flow regulator provides additional pressure drop to make up the difference between the total condenser pressure drop and its own frictional losses.

As depicted in Figure 1, the frictional pressure drop in each condenser is the sum of pressure drops in the two-phase and liquid-phase portions of the condenser, i.e.

$$(1)\ldots \quad \Delta P_C = \Delta P_{C,2\varphi}^{(i)} + \Delta P_{C,L}^{(i)} + \Delta P_{FR}^{(i)} \quad \text{for } i = 1 \text{ to } N_C$$

where both $\Delta P_{C,2\varphi}^{(i)}$ and $\Delta P_{C,L}^{(i)}$ are functions of the mass flow rate $\dot{m}_C^{(i)}$ and two-phase length $L_{C,2\varphi}^{(i)}$ of condenser

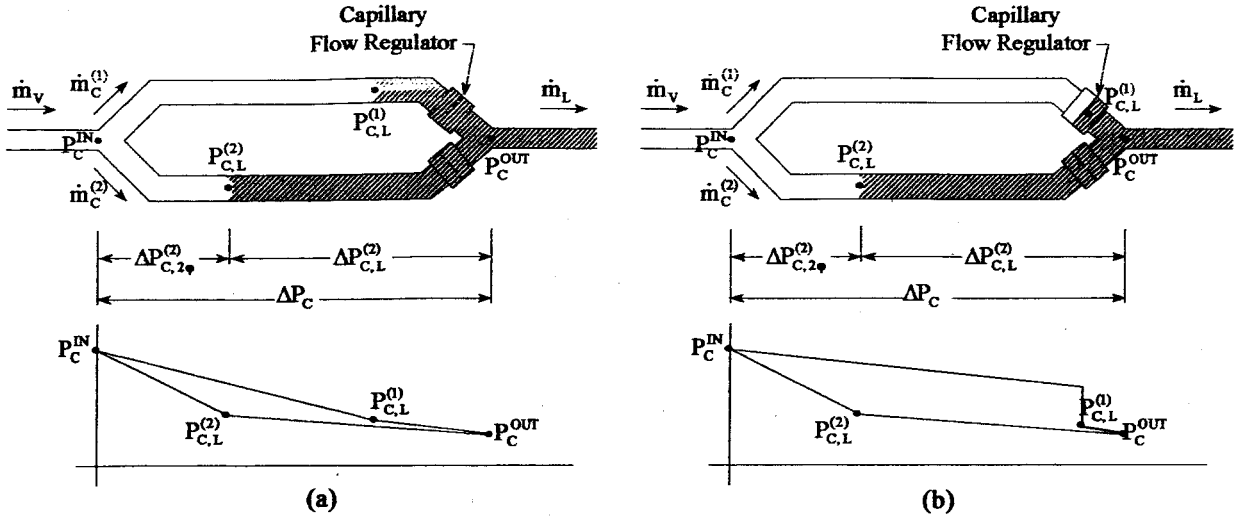

Figure 1 – Flow Distribution Among Parallel Condensers

i. Darcy's law for single-phase pipe flows is employed to calculate $\Delta P_{C,L}^{(i)}$ as follows:

$$(1a)\ldots\ \Delta P_{C,L}^{(i)} = -\frac{L_C^{(i)} - L_{C,2\varphi}^{(i)}}{D_C^{(i)}} f \frac{1}{2\rho}\left(\frac{\dot{m}_C^{(i)}}{A_C^{(i)}}\right)^2 \quad \text{for } i = 1 \text{ to } N_C$$

where,

$$f = \begin{cases} 64/Re & \text{laminar flow} \\ 0.316/Re^{1/4} & \text{turbulent flow} \end{cases}$$

For the two-phase pressure drop $\Delta P_{C,2\varphi}^{(i)}$, different two-phase models, depending upon the flow regime, can be used [8]. In each of these two-phase models, the heat transfer coefficient and pressure drop were correlated with respect to the local vapor void fraction, i.e.

$$(1b)\ldots\ \Delta P_{C,2\varphi}^{(i)} = -\int_0^1 \Phi_L^2 \frac{1}{D_C^{(i)}} f_{w,l} \frac{1}{2\rho_L}(1-x)^2 \left(\frac{\dot{m}}{A_C^{(i)}}\right)^2 \frac{1}{\left(\frac{dx}{dz}\right)} dx$$

where,

$$\left(\frac{dx}{dz}\right) = \frac{T_{SAT} - T_{SINK}}{\dot{m}_C^{(i)} \lambda} \pi D_C^{(i)} h_{2\varphi}$$

$$h_{2\varphi} = \Phi_L h_L$$

$$\Phi_L = \frac{1}{1-\alpha}$$

The two-phase length $L_{C,2\varphi}^{(i)}$ is also a function of the mass flow rate $\dot{m}_C^{(i)}$, i.e.

$$(2)\ldots\quad L_{C,2\varphi}^{(i)} = \frac{\dot{m}_C^{(i)} \lambda}{\pi D_C^{(i)} \left(T_{SAT} - T_{SINK}\right)} \int_0^1 \frac{1}{h_{2\varphi}} dx$$

From Eqs. (1), (1a), (1b) and (2), ΔP_C is an explicit function of $\dot{m}_C^{(i)}$, i.e.

$$(3)\ldots\quad \Delta P_C = F_i(\dot{m}_C^{(i)}) \qquad \text{for } i = 1 \text{ to } N_C$$

There are N_C equations in (3) for N_C+1 unknowns: $\dot{m}_C^{(i)}$ and ΔP_C. To close the problem, employ the continuity equation for the mass flow at the condenser inlet:

$$(4)\ldots\quad \sum_{i=1}^{N_C} \dot{m}_C^{(i)} = \dot{m}_V$$

Solving Eqs. (3) and (4) simultaneously will obtain the mass flow rates $\dot{m}_C^{(i)}$ in the parallel condensers. Note that when a condenser is fully open, vapor is prevented from flowing through that condenser by the capillary flow regulator. In other words, the flow regulator exerts an additional amount of capillary pressure to force the excess vapor to flow to other condensers as illustrated in Figure 1b.

PARALLEL CAPILLARY PUMPS

Referring to Figure 2, for a multiple parallel pump LHP to reach steady state, the following conditions must be satisfied:

$$(5)\ldots\quad \begin{cases} \dot{Q}_{2,MAX}^{(i)} = \dot{Q}_{SC,MAX}^{(i)} + \dot{Q}_{R\text{-}A}^{(i)} & \text{for } i = K \\ \dot{Q}_{2,MAX}^{(i)} \le \dot{Q}_{SC,MAX}^{(i)} + \dot{Q}_{R\text{-}A}^{(i)} & \text{for } i = 1 \text{ to } N_P \text{ and } i \ne K \end{cases}$$

Eq. (5) stipulates that the *worst-case* energy balance must be achieved for at least one of the pumps/hydro-

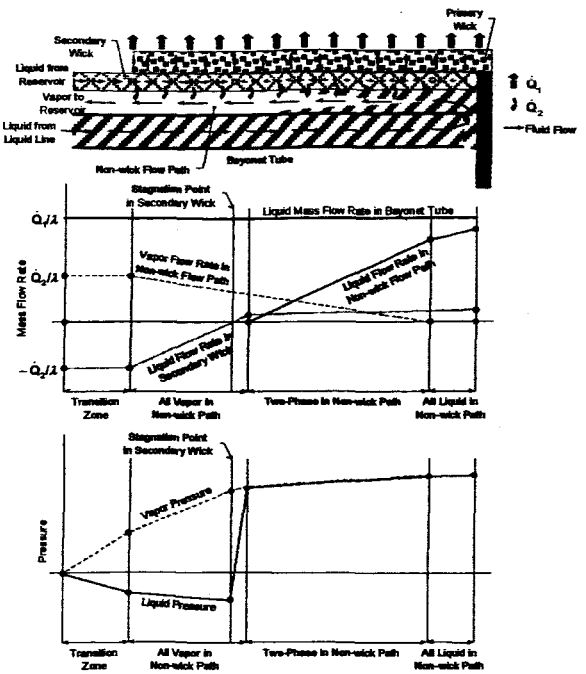

Figure 2 – Two-Phase Flow in Capillary Pump Core

accumulators (i.e. pump K). The worst-case heat leak condition occurs when both the hydro-accumulator and pump core contain both liquid and vapor. The heat leak $\dot{Q}^{(K)}_{2,MAX}$ and the amount of return subcooling $\dot{Q}^{(K)}_{SC,MAX}$ in pump K are:

(6)...

$$\dot{Q}^{(K)}_{2,MAX} = \frac{\dot{m}^{(K)}_P c_P}{(D^{(K)}_{O,W}/D^{(K)}_{I,W})^{\zeta} - 1} \Delta T^{(K)}_W \quad \text{with} \quad \zeta = \frac{\dot{m}^{(K)}_P c_P}{2\pi k^{(K)}_W L^{(K)}_W}$$

(7)... $$\dot{Q}^{(K)}_{SC,MAX} = \dot{m}^{(K)}_P c_P \left(T_{SAT} - T^{(K)}_{IN}\right)$$

Substituting Eqs. (6) and (7) into Eq. (5), will obtain:

(5a)... $$\frac{\dot{m}^{(K)}_P c_P}{(D^{(K)}_{O,W}/D^{(K)}_{I,W})^{\zeta} - 1} \Delta T^{(K)}_W = \dot{m}^{(K)}_P c_P \left(T_{SAT} - T^{(K)}_{IN}\right) + G^{(K)}_{R\text{-}A}(T_{SAT} - T_{\infty})$$

where,

$$\Delta T^{(K)}_W = \left(\frac{\partial T}{\partial P}\right)_{SAT} \Delta P^{(K)}_W$$

The total pressure drop across the pump wick $\Delta P^{(K)}_W$ depends strongly on the location of liquid-vapor front in the condenser, which in turn varies with the saturation temperature. Moreover, the thermo-physical properties of the working fluid are functions of temperature. Thus Eq. (5a) is usually solved iteratively to obtain the LHP operating temperature T_{SAT}.

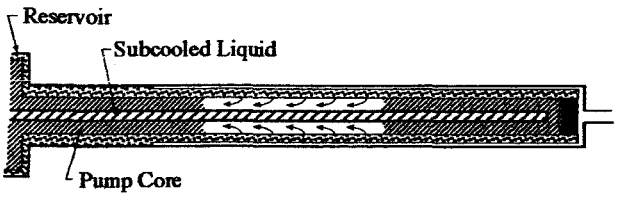

Figure 3 – Heat Leak Across LHP Wick

For other pumps, the energy balance is still met under a different condition. Starting with Eq. (5), when the heat leak $\dot{Q}^{(i)}_{2,MAX}$ is less than the combined cooling effect of $\dot{Q}^{(i)}_{SC,MAX}$ and $\dot{Q}^{(i)}_{R\text{-}A}$, then the vapor void fraction in the pump core and hydro-accumulator decreases, reducing *both* the heat leak $\dot{Q}^{(i)}_2$ and the return subcooling $\dot{Q}^{(i)}_{SC}$ as depicted in Figure 3. Note that the reduction of $\dot{Q}^{(i)}_{SC}$ is due to the incomplete heat exchange between the return subcooled liquid in the bayonet tube and the pump core vapor (i.e. the liquid exiting the bayonet is still subcooled). The vapor void fraction continues to decrease in pump i until it reaches a level at which the energy balance prevails. In other words, a two-phase condition may exist in the core and hydro-accumulator of pump i. However there is also a strong possibility that the pump core/hydro-accumulator is filled with liquid if the return subcooling overwhelms the heat leak in pump i.

In the steady state model, the worst-case heat leak is calculated to determine the LHP operating temperature $T^{(i)}_{SAT}$ that satisfies the energy balance of each pump, i.e.

(8)... $$\dot{Q}^{(i)}_{2,MAX} = \dot{Q}^{(i)}_{SC,MAX} + \dot{Q}^{(i)}_{R\text{-}A} \Rightarrow T^{(i)}_{SAT}$$

To achieve the system thermal equilibrium (or to satisfy Eq. (5)), the LHP operating temperature is the highest of all $T^{(i)}_{SAT}$. Or,

(9)... $$T_{SAT} = \max(T^{(i)}_{SAT}) \quad \text{for } i = 1 \text{ to } N_P$$

STEADY STATE COMPUTER CODE

A computer code, written in Visual BASIC, is used in conjunction with Microsoft Excel to predict the steady state operating temperature T_{SAT} of a multiple capillary pump/condenser LHP. For a given operating condition, the model goes through an iteration process to calculate T_{SAT} that satisfies Eq. (5). The iteration steps are described below:

(i) guess loop saturation temperature T^{GUESS}_{SAT}.
(ii) calculate thermo-physical properties (e.g. density, viscosity) of working fluid at T^{GUESS}_{SAT}.

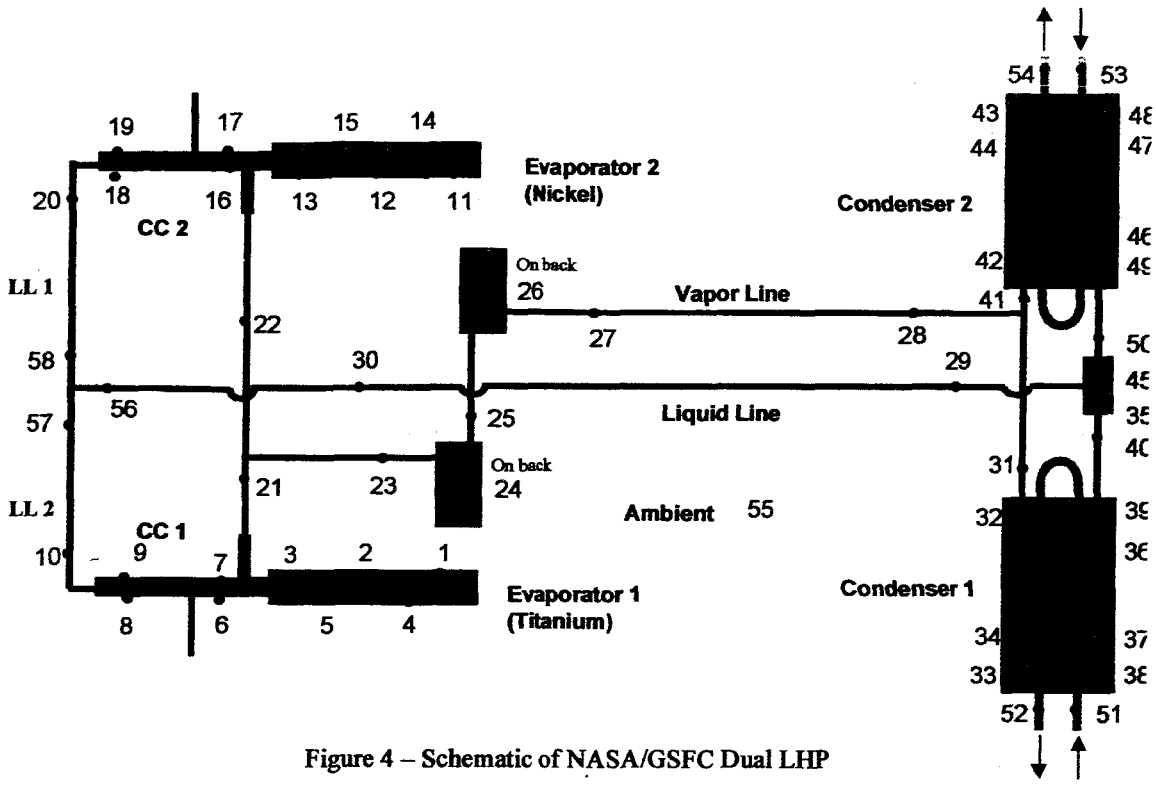

Figure 4 – Schematic of NASA/GSFC Dual LHP

(iii) solve Eq. (3) to determine heat removal/fluid flow distribution among parallel condensers.

(iv) calculate pressure drops in all LHP components to obtain total pressure drops across each pump wick.

(v) compute $\dot{Q}^{@}_{2,MAX}$, $\dot{Q}^{@}_{SC,MAX}$ from Eqs. (6) and (7) and $\dot{Q}^{@}_{R\text{-}A}$, then determine if the energy balance in pump i satisfies Equation/Inequality (5). If it does, exit iteration loop. Otherwise, go back to step (i) to repeat process until it does.

The loop saturation temperature is therefore regulated (or *controlled*) by the hydro-accumulator that satisfies the *Equation* (5) identically. As far as the steady state modeling is concerned, the exact thermodynamic states of the other hydro-accumulators are not required and therefore omitted in the current calculation. Note that the same cannot be said about the transient version of the LHP model in which the thermodynamic conditions of all hydro-accumulator had to be computed at every time step.

MODEL VERIFICATION

The verification of the LHP steady state computer code was made by correlating the model predictions versus available test data from a *dual* pump/condenser LHP as shown in Figure 4. The dual LHP test article, built by the Dynatherm Corporation, consisted of two parallel capillary evaporator pumps and two parallel condensers but shared common transport lines. Each evaporator pump had its own *concentric* hydro-accumulator. The evaporator casings were made of aluminum tubing having 15.8mm (5/8") O.D. and 76.2mm (3") length. The hydro-accumulators (14.8mm O.D. x 81.8mm L), machined from 316L stainless steel tubing, were welded to the evaporators by way of bi-metallic joints. One evaporator had a titanium wick and the other had a nickel wick. Properties of the wicks are summarized in Table 1.

Table 1 – Wick Properties of NASA/GSFC Dual LHP

Property	Titanium Wick	Nickel Wick
Pore Radius	3.0microns	0.6microns
Porosity	45%	60%
Permeability	$7.4\times10^{-14}m^2$	$1.4\times10^{-14}m^2$
Thermal Conductivity	7.2W/m-K	5.8W/m-K

The vapor and liquid lines were made of stainless steel tubing, having the respective outer diameters of 2.2mm (3/32") and 1.6mm (1/16"). The length of both vapor and liquid lines measured approximately 1,168mm (46"). Each condenser was formed by sandwiching a serpentine 2.2mm O.D. x 1,016mm L stainless steel line between two 82.6mm x 177.8mm (3.25"x7") aluminum plates. A flow regulator made of 20μm-pore capillary screens was placed downstream of the condensers. The flow regulator prevented vapor from returning to the evaporator pumps when one of the condensers was fully

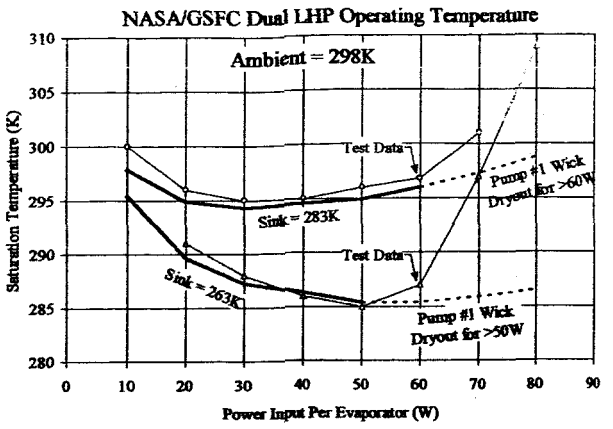

Figure 5 – Model Predictions vs. Test Data

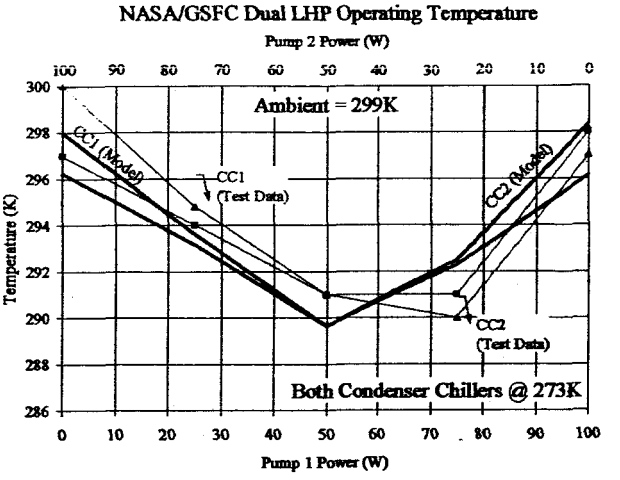

Figure 6 – Model Predictions vs. Test Data

utilized, and hence served to balance the fluid flow between the two condensers. The loop was charged with 15.5 grams of anhydrous ammonia.

Electrical heaters were attached to both evaporators and hydro-accumulators and the heater power inputs were regulated by separate power supplies. The two condensers were clamped to two cold plates; each cooled by a chiller. Sixty thermocouples were used to monitor the loop temperatures. Notice that many thermocouples were installed on the liquid line between the two hydro-accumulators in order to detect any interaction between the two during fast transients. A data acquisition system consisting of a data logger, a personal computer, a CRT monitor, and Labview software was used to monitor and store data. The data was updated on the monitor and stored in the computer every second.

Figure 5 presents the temperature comparison between the test data and model predictions for the case in which the same heater power was applied to each evaporator pump. In the tests, two sink conditions (–10°C and +10°C) were imposed on the loop operation. The correlation was excellent. The operating temperature from the model simulation came within ±2°C of the test data in this test series when the power input was less than 60W/pump for the +10°C sink and 50W/pump for the –10°C sink. For power inputs higher than these levels, the model showed that the system pressure drop exceeded the capillary limit of the titanium wick. Note that this condition only implied that vapor vented into the pump core through some area of the wick (partial dryout) but might not necessarily lead to a complete dryout of the titanium wick (i.e. pump #1 deprime). Nevertheless the actual LHP saturation temperature was progressively higher than those predicted by the model as the power input increased beyond 60W/pump. In other words, even though pump #1 did not fail, the vapor leakage through the wick had the same effects as the heat leak $\dot{Q}_2^{@}$. Both test data and model predictions indicated that the hydro-accumulator #1 of the titanium wick pump actually *controlled* the loop saturation temperature. This made perfect sense, since the titanium wick has a higher effective thermal conductivity than that of the nickel wick, resulting in a higher amount of heat leak $\dot{Q}_2^{@}$ into the hydro-accumulator #1. Under the same heat input, each pump drew about the same amount of return liquid subcooling $\dot{Q}_{SC}^{@}$. Thus according to Eq. (5), the hydro-accumulator #1 had to drive the LHP to a higher temperature to satisfy its energy balance.

Figure 6 shows the test results and model predictions of the *uneven* power tests. During this series of tests, both sink (condenser) temperatures were set at 0°C. The power inputs to the evaporators were varied with a 25W increment but the combined power was maintained at 100W. As expected, the evaporator that had less heat input controlled the loop saturation temperature (since it drew less subcooling $\dot{Q}_{SC}^{@}$ back to the pump). The model prediction of the loop saturation temperature was also very good for the uneven power tests. In addition, it correctly predicted the hydro-accumulator that controlled the LHP temperature for a given condition.

CONCLUSIONS

Loop Heat Pipes have become increasingly popular with spacecraft thermal engineers for their operational reliability and robustness. Well over 100 conventional LHPs have been utilized for spacecraft Thermal Control Systems (TCS). Thus multiple evaporator/condenser LHPs are the next logical step in the LHP utilization. Indeed several flight projects are considering them as

the primary TCS. Appropriately, the thermal engineers need accurate LHP models to simulate the thermal system performance particularly on-orbit behaviors.

The LHP theory of conventional LHP operation was extended to multiple pump/condenser systems, and from which, a steady state computer code was written. The computer code was simple and easy to use. As presented in this paper, the computer predictions agreed well with available test data. Nevertheless, the modeling effort should continue to provide a better simulation tool for space applications especially in transient predictions.

REFERENCES

[1] Bienert, W., and D. Wolf, "Temperature Control with Loop Heat Pipes: Analytical Model and Test Results," *Proceedings of the 9th International Heat Pipe Conference*, Los Alamos National Laboratory, May 1995.

[2] Kaya, T., J. Ku, T. Hoang, and M. Cheung, "Mathematical Modeling of Loop Heat Pipes," Paper No. AIAA 99-0477, 1999.

[3] Kaya, T. and T. Hoang, "Mathematical Modeling of Loop Heat Pipes and Experimental Validation," Journal of Thermophysics and Heat Transfer, Volume 13, Number 3, July-September 99.

[4] Hoang, T., "Transient Modeling of Loop Heat Pipes," Two-Phase Technology '99, Workshop on Ambient and Cryogenic Thermal Control Devices, University of Maryland College Park, Maryland, May 17-19, 1999.

[5] Wrenn, K., and T. Hoang, "Verification of a Transient Loop Heat Pipe Model," SAE Paper 99ES-92, 29th International Conference on Environmental Systems, Denver, CO, July 1999.

[6] Hoang, T. and J. Ku, "Transient Modeling of Loop Heat Pipes," Paper No. AIAA 2003-6082, 1st IECEC, August 17-21, 2003, Portsmouth, Virginia.

[7] Hoang, T., K. Cheung, and R. Baldauff, "Loop Heat Pipe Testing and Analytical Model Verification at the U.S. Naval Research Laboratory," Paper No. 04ICES-288, 34th ICES, 2004, Colorado Springs, CO.

[8] Izenson, M.G. and C.J. Crowley, "Design of Condensing Radiators for Spacecraft Thermal Management," AIAA Paper No. A92-47847, AIAA 27th Thermophysics Conference, Nashville, TN, July 6-8, 1992.